SEISMIC RESPONSE STUDY OF THE US 101/ PAINTER STREET OVERPASS USING STRONG MOTION RECORDS

Rakesh K. Goel and Anil K. Chopra

Department of Civil Engineering
University of California at Berkeley

ABSTRACT

Abutment stiffnesses are determined directly from the earthquake motions recorded at the US 101/ Painter Street Overpass using a simple equilibrium-based approach without finite-element modeling of the structure or the abutment-soil systems. The calculated abutment stiffnesses, which include the effects of soil-structure interaction and nonlinear behavior of the soil, are used to investigate variation of the abutment stiffness with its deformation during the earthquake and torsional motions of the road deck. Also evaluated are the CALTRANS, ASSHTO-83, and ATC-6 procedures for estimating the abutment stiffness. It is demonstrated that stiffness of the abutment depends significantly on its deformation during the earthquake: larger is the deformation, smaller is the stiffness. The road deck of this structure experienced significant torsional motions in part because of eccentricity created by different transverse stiffnesses at the two abutments. It is also shown that the CALTRANS procedure leads to good estimate of the abutment stiffness provided the deformation assumed in computing the stiffness is close to actual deformation during the earthquake, and ASSHTO-83/ATC-6 procedure results in stiffer initial estimate of the abutment stiffness.

INTRODUCTION

The 1971 San Fernando earthquake clearly demonstrated the importance of abutment-soil systems in earthquake response of short bridges (Jennings and Wood, 1971). Recognizing this importance, most earthquake design codes for highway bridges require that the abutment-soil systems be included in the structural idealization as equivalent discrete springs (CALTRANS, 1990; ATC-6, 1981; AASHTO-83, 1988). Needed for such code-based earthquake analyses of short bridges are the stiffness values of the abutment-soil springs. In the design profession, these values are selected based on some simplified rules and trial-and-error process. It is not entirely clear how well the stiffness values thus determined represent the complex behavior of the abutment-soil systems, such as soil-structure interaction and nonlinear behavior of the soil, during actual ground shaking. It is therefore important to determine the stiffness values directly from the motions recorded during actual earthquakes.

This investigation is aimed at filling this need. The primary objective of this investigation is to determine the stiffness values of the abutment-soil systems from the earthquake motions recorded at the US 101/ Painter Street Overpass without any finite-element modeling of the structure or abutment-soil systems. The approach adopted in this investigation involves estimating the stiffness

of the abutment-soil systems from their force-deformation loops, which are determined from the recorded motions using the dynamic equilibrium of the road deck. This simple approach is possible because the US 101/ Painter Street Overpass can be idealized by just a few stiffness parameters -- springs along the east abutment, normal to the east abutment, and along the west abutment; for simplicity, the stiffness values of two columns in the central bent are assumed to be known and are determined from their structural details. The calculated abutment stiffnesses, which include the effects of soil-structure interaction and nonlinear behavior of the soil, are used to investigate variation of the abutment stiffness with its deformation during the earthquake and torsional motions of the road deck of this structure. Also evaluated are the CALTRANS, ASSHTO-83, and ATC-6 procedures for estimating the abutment stiffness.

STRUCTURE AND RECORDED MOTIONS

Identified as CSMIP Station No. 89324, the US 101/ Painter Street Overpass (Figure 1) is located in Rio Dell, California. This 265 ft long bridge consists of a continuous reinforced-concrete (R/C) multi-cell box-girder road deck supported on integral abutments at the two ends and on an R/C two-column bent, which divides the bridge into two unequal spans of 119 ft and 146 ft. Both abutments and bent are skewed at an angle of 38.9°. The east abutment is supported on 14 driven 45-ton concrete friction piles. The west abutment rests on a neoprene bearing strip that is part of a designed thermal expansion joint of the road deck. The foundation of this abutment consists of 16 driven 45-ton concrete friction piles. This bridge is typical of short bridges in California spanning two or four lanes separated highways.

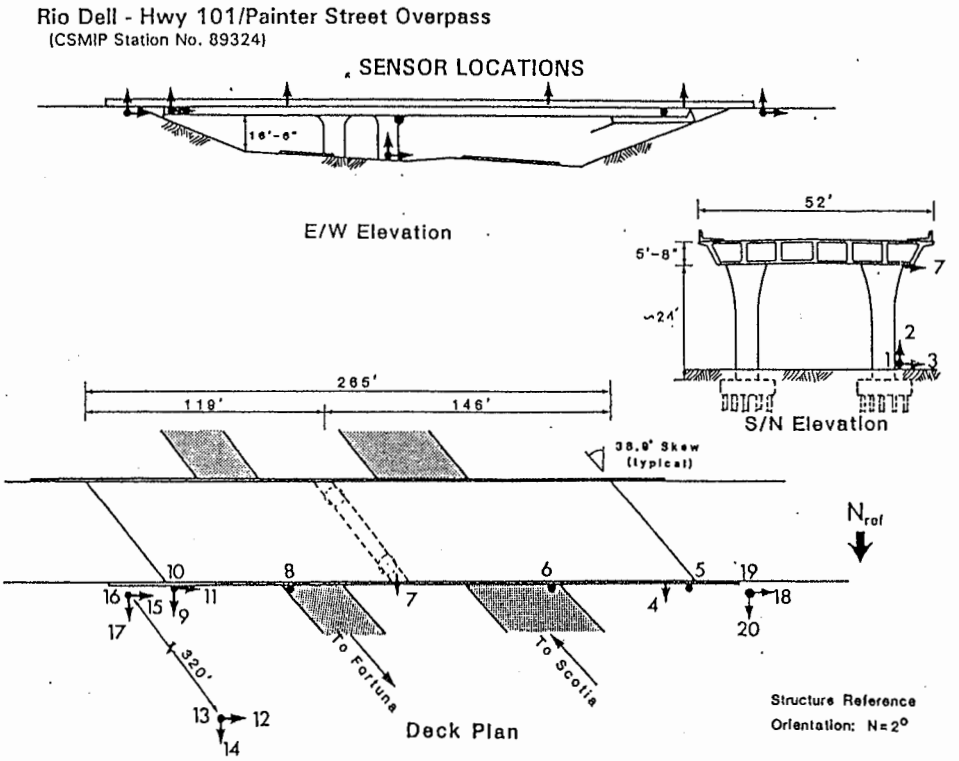

Figure 1. US 101/ Painter Street Overpass (Shakal et al., 1992)

The US 101/ Painter Street Overpass was instrumented by California Strong Motion Instrumentation Program (CSMIP) in 1977. Figure 1 shows locations of the instruments and identifies the channels on this structure. Since this overpass was instrumented, it has yielded strong motion records during nine earthquakes (Table 1). For the purpose of this research investigation, we have selected motions recorded during two earthquakes: the main shock of the April 25, 1992, Cape Mendocino/ Petrolia earthquake which produced the maximum free-field acceleration of 0.543g that was amplified to 1.089g at the structure; and the second event of the November 21, 1986, Cape Mendocino earthquake that caused much smaller motions of 0.144g and 0.35g at the free-field and the structure, respectively.

Table 1. List of recorded motions at the US 101/ Painter Street Overpass

No.	Earthquake	Depth (Km.)	Mag. M_L	Dist. (Km.)	Max. FF Acc. (g)	Max. Str. Acc. (g)
1.	Trinidad Offshore 8 Nov, 1980	19	6.9	82	0.147	0.169
2.	Rio Dell 16 Dec, 1982	5	4.4	15	--	0.420
3.	Eureka 24 Aug, 1983	30	5.5	61	--	0.215
4.	Cape Mendocino 21 Nov, 1986 (First Event)	17	5.1	32	0.432	0.399
5.	Cape Mendocino 21 Nov, 1986 (Second Event)	18	5.1	26	0.144	0.350
6.	Cape Mendocino 31 Jul, 1987	17	5.5	28	0.141	0.335
7.	Cape Mendocino/ Petrolia Apr 25, 1992	15	6.9	6.4	0.543	1.089
8.	Cape Mendocino/ Petrolia Apr 26, 1992 (AS # 1)	18	6.2	6.2	0.516	0.757
9.	Cape Mendocino/ Petrolia Apr 26, 1992 (AS # 2)	21	6.5	6.4	0.262	0.311

ANALYSIS PROCEDURE

Structural Idealization

Figure 2 shows the free-body diagram of an idealized model of the US 101/ Painter Street Overpass. The model consists the road deck with three spring-dampers, which represent the abutment-soil systems along the east abutment, normal to the east abutment, and along the west abutment. The spring represents the stiffness of the abutment and the damper accounts for material and radiation damping of the abutment-soil system. Each column in the central bent is represented by two simple linear elastic springs -- one normal to and other along the bent. The stiffness values of these springs are computed by frame analysis of the bent using the cracked stiffness of each column with inertia values determined from its moment-curvature relationship.

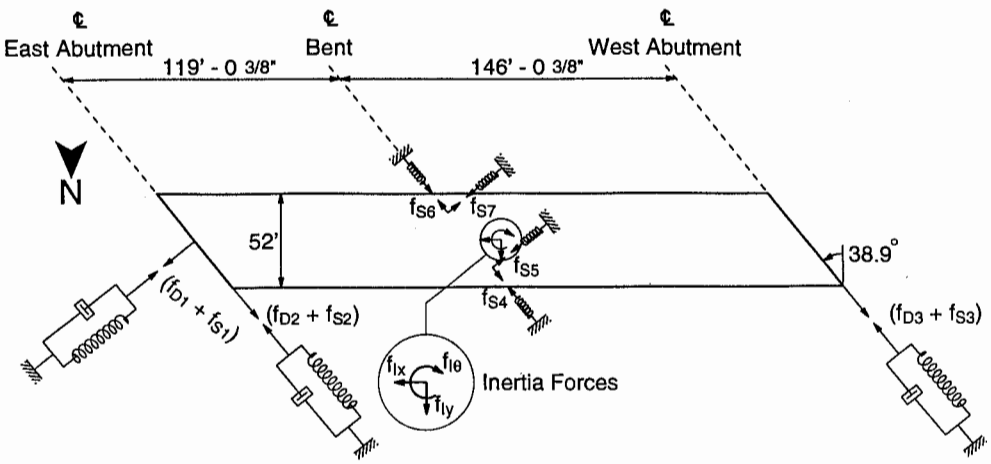

Figure 2. Free-body diagram of an idealized model of US 101/ Painter Street Overpass

Equations of Equilibrium

The three equations of dynamic equilibrium for the system of Figure 2 are:

$$f_I + f_D + f_S = 0 \qquad (1)$$

in which $f_I^T = \langle f_{Ix},\ f_{Iy},\ f_{I\theta} \rangle$ is the vector of inertia forces, f_D is the vector of damping forces, and f_S is the vector of spring forces; f_D and f_S are formed by transforming forces at the abutments -- $(f_{D1}+f_{S1})$, $(f_{D2}+f_{S2})$, and $(f_{D3}+f_{S3})$; and the forces at the columns -- f_{S4}, f_{S5}, f_{S6}, and f_{S7}.

Abutment Forces and Deformations

The only unknowns in equation (1) are the abutment forces, which are determined by solving the three equations at each instant of time. The three components of the inertia force vector are computed from the mass properties, determined from the structural plans, and recorded accelerations. The force in each column spring is determined from its known stiffness and deformation.

At each time-instant, the deformation in the spring-damper system, modeling the abutment-soil system, or the column spring is obtained by subtracting the free-field motion from the motion at the top of the abutment or the column; the latter can be computed from recorded motions of the road deck.

Abutment Stiffness

If the computed abutment force is plotted against its calculated deformation for many time instances, we will obtain hysteresis loops. The abutment stiffness is calculated from these hysteresis loops as described next. The force-deformation hysteresis loops are generated for the selected earthquakes. The stiffness of each of the abutment-soil systems is determined by isolating individual loops. Three such loops -- one for each of the three abutments -- are shown in Figure 3.

The somewhat elliptical shape of the loop for the spring normal to the east abutment (Figure 3a) suggests elastic behavior. From such a loop the spring stiffness is obtained by selecting its slope as shown by the two straight lines; the corresponding values are 29768 and 23500 kips/ft. Although the loop for the spring along the east abutment (Figure 3b) deviates considerably from a

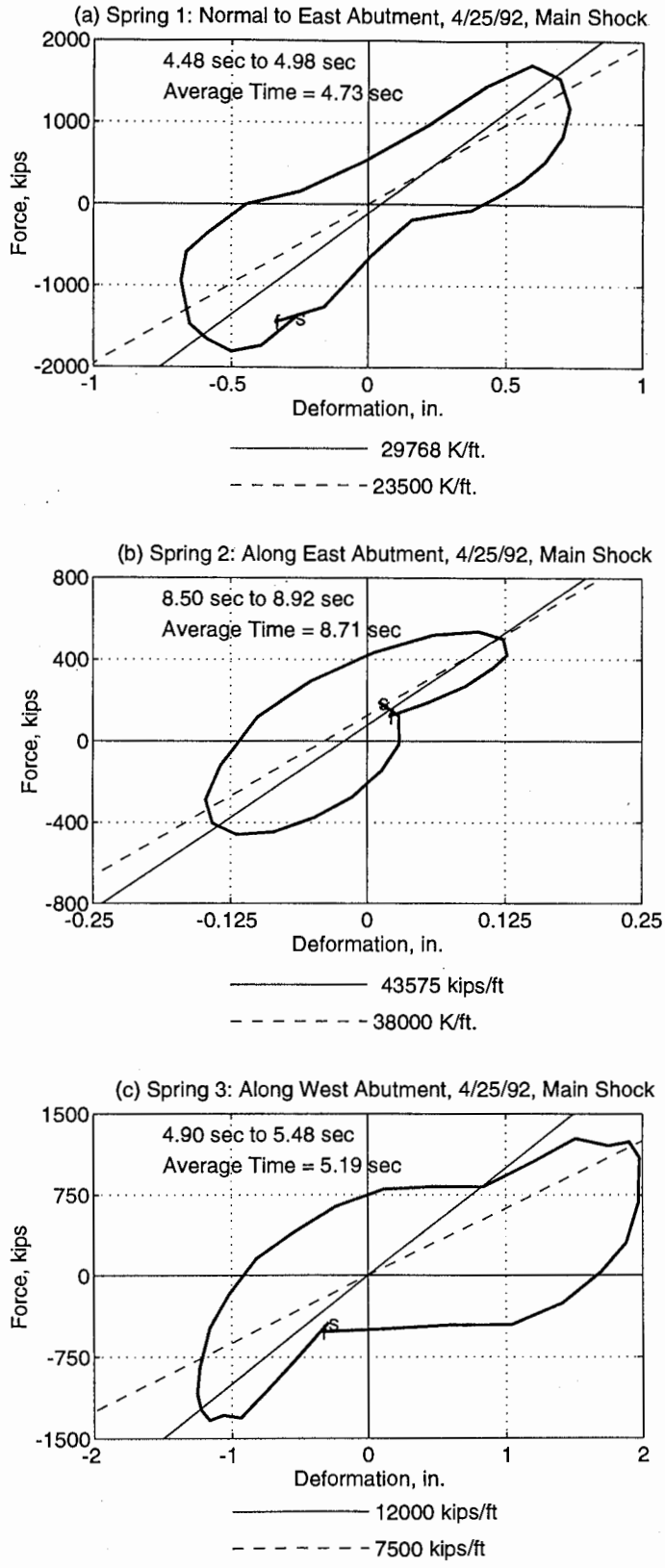

Figure 3. Selected force-deformation hysteresis loops

perfect ellipse, it is still possible to estimate the stiffness value for this spring; the upper and lower bound values in this case are 43575 and 38000 kips/ft.

Unlike the two previous loops, which suggest elastic behavior of the springs, the loop selected for the spring along the west abutment (Figure 3c) exhibits significant non linearity as evident from the elasto-plastic with strain hardening force-deformation behavior. From such loops, the upper and lower bounds of the stiffness are obtained by selecting the secant stiffness values; these values are 7500 and 12000 kips/ft for the positive and negative deformations, respectively.

Such results are used next to investigate variation of the abutment stiffness with its deformation during the earthquake. For this purpose, the time-variation of the stiffness during the larger earthquake is examined first. Subsequently, abutment stiffness values are compared for the two selected earthquakes. Also compared are the transverse stiffness values of the two abutments to explain the torsional motions of the road deck during the large earthquake.

TIME-VARIATION OF ABUTMENT STIFFNESS

Figure 4 shows the time-variation of stiffness for the three abutments during the main shock of the 1992 Cape Mendocino/ Petrolia earthquake. Since the stiffness value is the average stiffness over the time duration of one loop, it is shown as a discrete point plotted at the middle of this duration. It is clear from these results that the abutment stiffness varies significantly during the same earthquake. This variation is particularly large for the spring normal to the east abutment (Figure 4a). In order to further investigate this behavior of the abutment, plotted on the right vertical axis of Figure 4 is its total deformation, which is the sum of the deformation amplitudes in the positive and negative directions. By examining the deformations along with the stiffnesses, the following general pattern emerges.

- The abutment tends to be stiff for small deformation such as during the build-up phase of the shaking (first set of values in Figures 4a and 4b).
- The abutment stiffness reduces with its increasing deformation as the amplitude of the motion increases during the strong motion phase (values between 5 and 9 sec in Figures 4a to 4c).
- The abutment recovers some of its stiffness with subsequent reduction in its deformation as the motion becomes less intense towards the later part of the shaking (values after 10 sec in Figures 4a and 4c).
- The recovery of abutment stiffness is only partial: the stiffness for a deformation level may not return to the value prior to a large deformation cycle. This recovery is gradual over time and is especially slow after repeated large deformation cycles (Figure 4a).

This abutment behavior indicates that soil enclosed between the wingwalls provides significant resistance to the abutment motion for small deformation levels. For large deformations, however, the soil becomes less effective. The reduction in stiffness for large deformation may also be due to nonlinear behavior of the soil (Figure 3c).

COMPARISON OF ABUTMENT STIFFNESS DURING TWO EARTHQUAKES

Compared in Figure 5 are the abutment stiffness values during the second event of 1986 Cape Mendocino earthquake and the main shock of 1992 Cape Mendocino/ Petrolia earthquake. Since

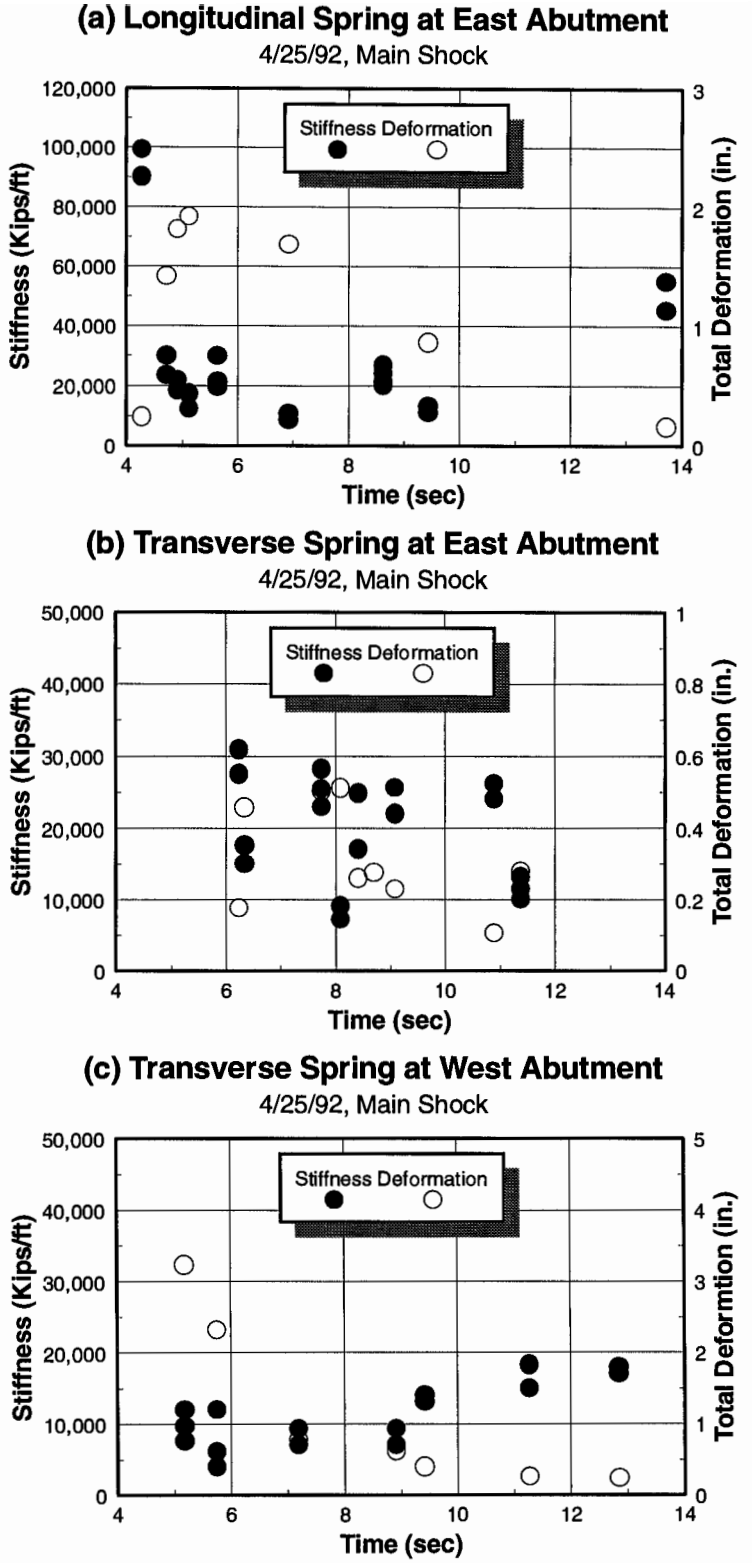

Figure 4. Time-variation of abutment stiffness and deformation

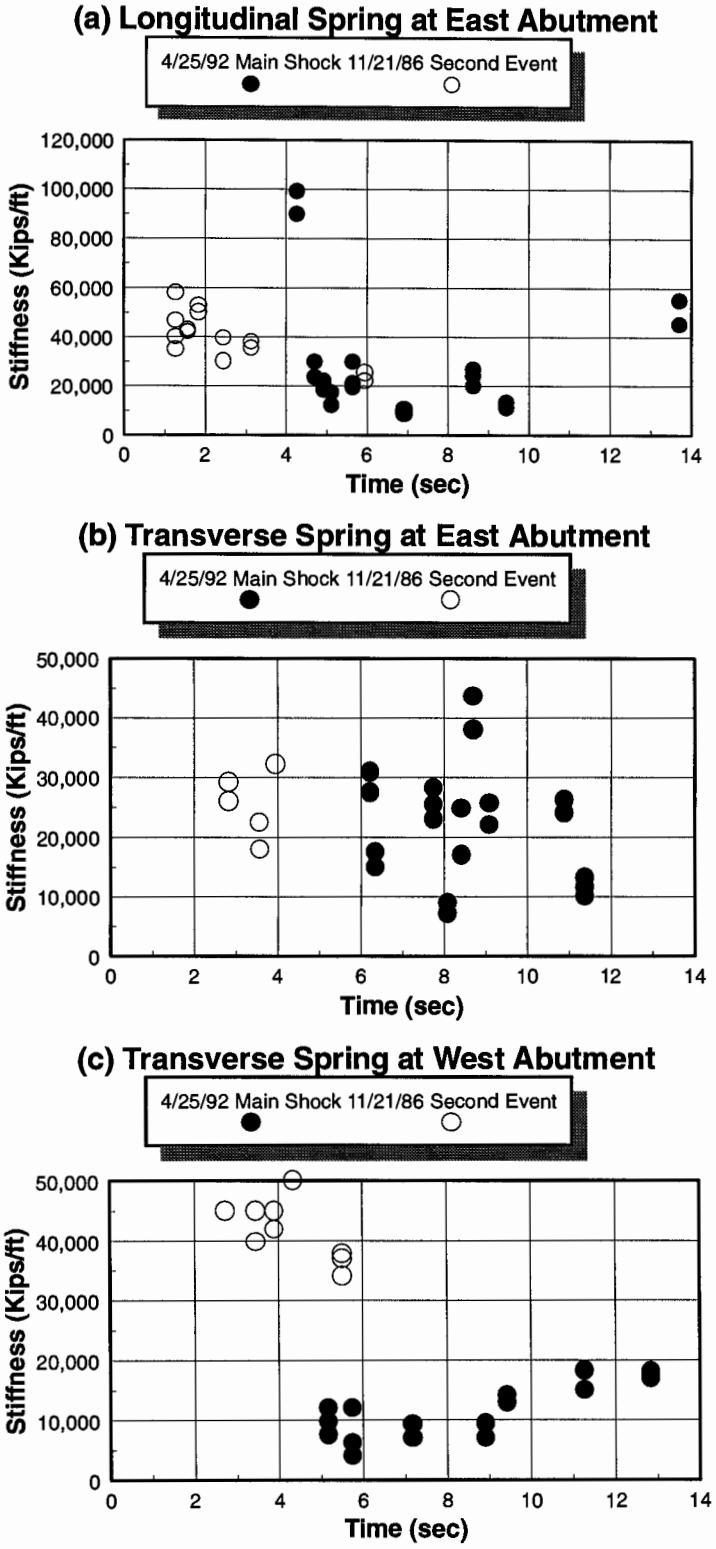

Figure 5. Comparison of stiffness for two earthquakes

the duration of shaking and amplitudes of motion are smaller for former of these two earthquakes, only a few stiffness values during the strong shaking phase are identified; many more stiffness values spread over all the three phases are available for the latter earthquake. These results show that trends in the abutment behavior are consistent with the trends identified in the previous section. The abutment is in general less stiff during the latter of the two earthquakes (Figures 5a and 5c) because of larger abutment deformations resulting from more intense shaking during this earthquake. For the purpose of this comparison, abutment deformations similar to those shown in Figure 4 for the 1992 earthquake were also computed for the 1986 earthquake but are not included here for brevity. This effect is more pronounced for the west abutment because of its larger deformations resulting from torsional motions of the road deck during the 1992 earthquake (Figure 5c). For similar deformations during the two earthquakes, such as those in the transverse direction at the east abutment, the abutment stiffnesses are also similar (Figure 5b).

TORSIONAL MOTIONS OF THE ROAD DECK

The road deck of the US 101/ Painter Street Overpass experienced significant torsional motions about its vertical axis during the main shock of the 1992 Cape Mendocino/ Petrolia earthquake; peak acceleration at the west end of the road deck was more than one-and-a-half times the value at the east end during this earthquake. In order to investigate the cause of this behavior of the road deck, the transverse stiffnesses of the two abutments (Figures 4b and 4c) are compared in Figure 6. The transverse stiffness of the west abutment is significantly smaller compared to the east abutment because of several reasons. The two abutments are of the same size but the west abutment is taller and hence less stiff. Furthermore, the east abutment is constructed monolithic with the footing while the west abutment is seated on a neoprene bearing to permit thermal movement that introduces additional flexibility at the west abutment. The center of rigidity of the deck would be closer to stiffer of the two abutments, the east abutment, whereas the center of mass would be located close to midway between the two abutments. The resulting eccentricity between the centers of mass and rigidity contributed to the torsional motion of the deck. As shown earlier (Goel and Chopra, 1990), the motion should be larger on the flexible side, the west abutment, and this is consistent with the recorded motions.

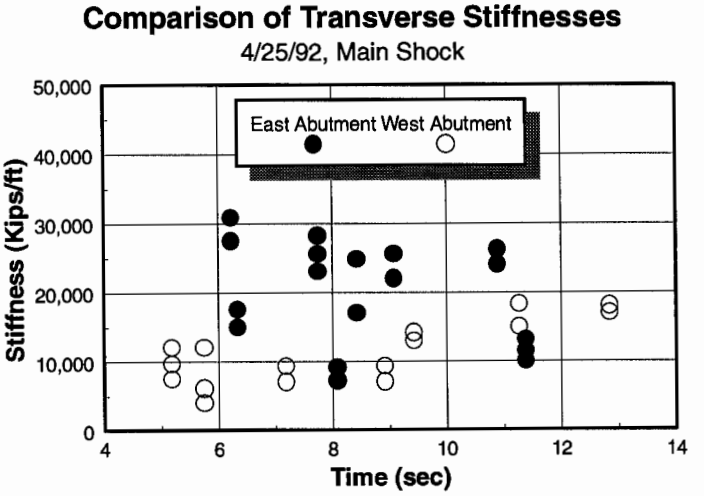

Figure 6. Comparison of transverse stiffnesses of the east and west abutments

EVALUATION OF CURRENT PROCEDURES

Compared in Figure 7 are the abutment stiffness values determined from recorded motions (Figures 4 to 6) with the values computed by CALTRANS, AASHTO-83, and ATC-6 procedures; the ASSHTO-83 and ATC-6 values are identical. Also included are values determined by Gates and Smith (1982) and Romstad and Maroney (1990). The results presented are for the main shock of the 1992 Cape Mendocino/ Petrolia earthquake.

The stiffness values for the CALTRANS procedure are determined from the abutment capacity (CALTRANS, 1988) in conjunction with the acceptable deformation. Two values of the acceptable deformation are considered: 1 inch and 2.4 inch; the former corresponds to the limit when the soil pressure behind the backwall of the abutment reaches its maximum value of 7.7 ksf, and the latter corresponds to the limiting value for avoiding damage to the abutment (CALTRANS, 1988, 1989). Note that the iterative procedure in which the initial stiffness is computed by assuming the soil stiffness of 200 kips/in per linear foot of the abutment backwall or wingwall (Tsai et al., 1993; CALTRANS, 1990) is not included in this investigation because CALTRANS engineers no longer consider this as a preferred procedure.

Table 2 shows the computed abutment stiffnesses using the above-described procedure. For computing longitudinal stiffness, several possibilities are considered. First two correspond to resistance provided only by one abutment such as before closure of the expansion joint gap or after failure of the shear key at the west abutment. The other two correspond to resistance provided by both the abutments when the shear key is engaged at the west abutment. Two possible failure modes are considered to calculate the backwall capacity: shear failure in the backwall just below the road deck soffit before the piles fail, and the failure of piles before the backwall fails. In each case, the soil depth equal to the road deck is considered for computing the soil resistance (CALTRANS, 1988). The transverse stiffness is based on the shear capacity of one wingwall and foundation capacity; the foundation capacity for the east abutment is selected as the capacity of the piles whereas that for the west abutment it is taken as the capacity of the shear key, which is assumed to be 0.75 times the capacity of the piles.

Figure 7a shows that the longitudinal stiffness computed by the CALTRANS procedure with 2.4 inch deformation matches quite well with values during the strong shaking phase of the earthquake. The exceptions occur during the build-up phase and towards the end of the earthquake where the abutment stiffness may be significantly larger than the CALTRANS values. This occurs because the abutment deformations during these phases of the earthquake are much smaller than 2.4 inch assumed in calculating the CALTRANS values. For obvious reasons, the CALTRANS values for 1 inch abutment deformation are significantly higher compared to values during strong shaking phase of the earthquake.

Since the stiffness computed by the ASSHTO-83/ATC-6 procedure is an initial estimate, it is larger than the values during the earthquake; it is expected that the final value obtained by the iterative procedure would be closer to the values during the earthquake. The stiffness determined by Gates and Smith is significantly higher because this value is determined for lower deformation levels (ambient vibration). Since Romstad and Maroney suggested that the abutment is rigid (infinitely stiff) in this direction, their value is not included.

Results for the transverse stiffness show that the east abutment in general remained much stiffer during the earthquake compared to the CALTRANS values for both deformation levels -- 1 inch and 2.4 inch -- and ASSHTO-83/ATC-6 value (Figure 7b). This difference can be explained

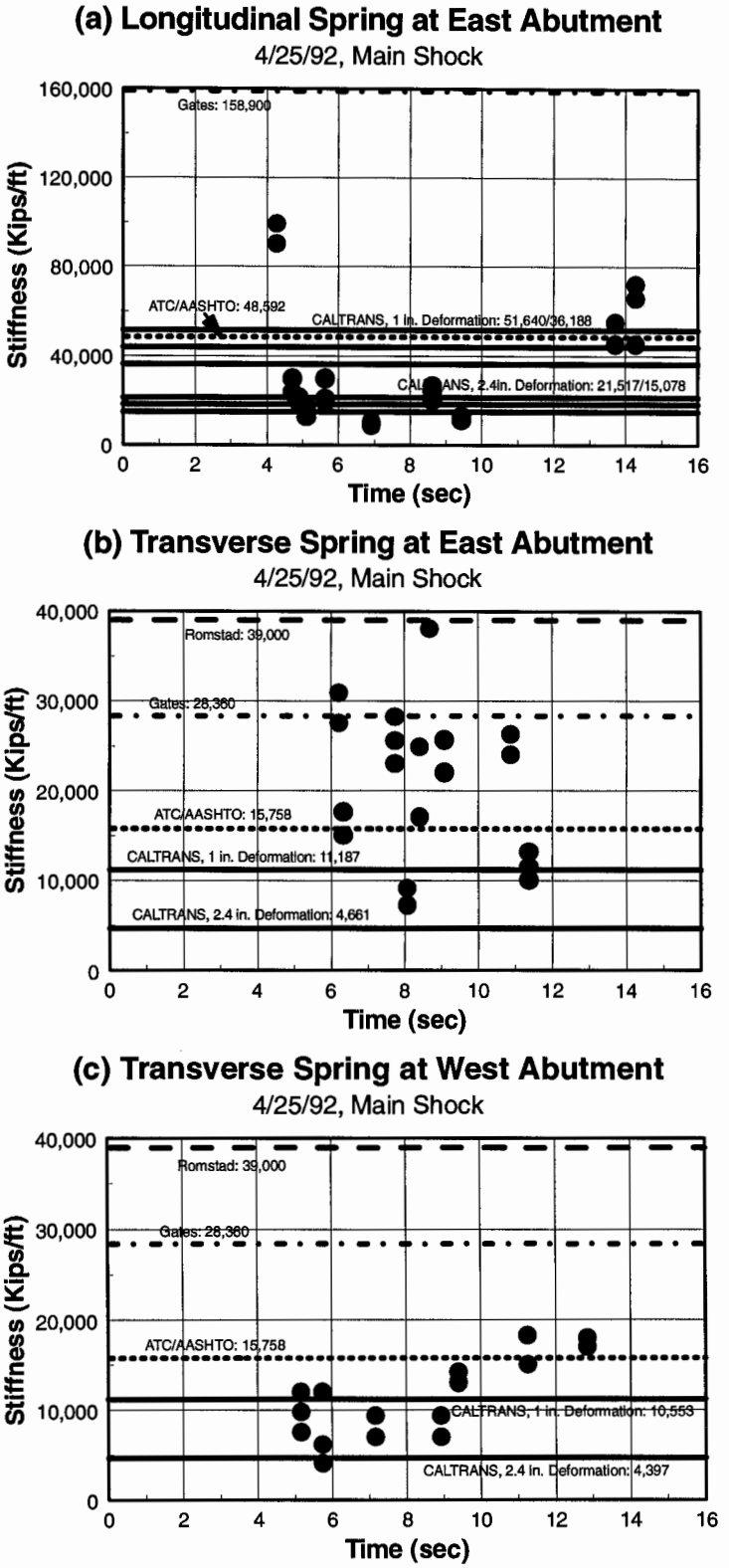

Figure 7. Comparison of abutment stiffness values determined from recorded motions with the values computed using the current procedures

Table 2. Abutment stiffness from CALTRANS procedures

Direction	Stiffness (kips/ft)	Assumptions
Longitudinal	43,960	$EQ_L = R_{SOIL} + V_{DIAPHRAGM}$, Deformation ≤ 1 inch.
	36,188	$EQ_L = R_{SOIL} + R_{PILES,\ ONE\ ABUT.}$, Deformation ≤ 1 inch.
	51,640	$EQ_L = R_{SOIL} + V_{DIAPHRAGM} + R_{PILES,\ ONE\ ABUT.}$, Deformation ≤ 1 inch.
	43,868	$EQ_L = R_{SOIL} + R_{PILES,\ BOTH\ ABUT.}$, Deformation ≤ 1 inch.
	18,317	$EQ_L = R_{SOIL} + V_{DIAPHRAGM}$, Deformation = 2.4 inch.
	15,078	$EQ_L = R_{SOIL} + R_{PILES,\ ONE\ ABUT.}$, Deformation = 2.4 inch.
	21,517	$EQ_L = R_{SOIL} + V_{DIAPHRAGM} + R_{PILES,\ ONE\ ABUT.}$, Deformation = 2.4 inch.
	18,278	$EQ_L = R_{SOIL} + R_{PILES,\ BOTH\ ABUT.}$, Deformation = 2.4 inch.
Transverse East	11,187	$EQ_T = V_{WW} + R_{PILES}$, Deformation ≤ 1 inch.
	4,661	$EQ_T = V_{WW} + R_{PILES}$, Deformation = 2.4 inch.
Transverse West	10,553	$EQ_T = V_{WW} + 0.75 R_{PILES}$, Deformation ≤ 1 inch.
	4,397	$EQ_T = V_{WW} + 0.75 R_{PILES}$, Deformation = 2.4 inch.

by noting that the earthquake-induced deformations are significantly smaller compared to those assumed in calculating the code values. The stiffness tends to be close to the value determined by Gates and Smith from low-level vibration but smaller than the value suggested by Romstad and Maroney based on smaller earthquakes. For the west abutment, the CALTRANS values for the two deformation levels form the upper and lower bounds of its stiffness during strong shaking phase (Figure 7c). Since the deformations of this abutment during the strong shaking phase of the earthquake are in the range of 1 to 2.4 inch, it appears that the CALTRANS procedure leads to good estimate of the abutment stiffness. During the decaying phase, however, the stiffness values may be higher than both the CALTRANS values because of much smaller deformation of the abutment. The ASSHTO-83/ATC-6 value tends to be higher than the earthquake value. Since the values determined by Gates and Smith (1982) and Romstad and Maroney (1990) are both for smaller deformation levels, these values tend to be much higher than the values during the earthquake.

CONCLUSIONS

In this investigation, abutment stiffnesses are determined directly from the recorded earthquake motions of the US 101/ Painter Street Overpass using a simple equilibrium-based approach without finite-element modeling of the structure or the abutment-soil systems. The values determined in this manner include the effects of soil-structure interaction and nonlinear behavior of the soil. Using these values, this investigation on variation of the abutment stiffness with its deformation during the earthquake and torsional motions of the road deck of this structure has led to the following conclusions. The abutment stiffness may be significantly

different during different phases of the shaking and depends on its deformation: larger is the deformation, smaller is the stiffness. The road deck of this structure experienced significant torsional motions in part because of eccentricity created by different transverse stiffnesses at the two abutments. Evaluation of the current modeling procedures for abutment stiffness indicates that the CALTRANS procedure leads to good estimate of the abutment stiffness provided the deformation assumed in computing the stiffness is close to actual deformation during the earthquake, and ASSHTO-83 and ATC-6 result in stiffer initial estimate of abutment stiffness.

ACKNOWLEDGMENTS

This investigation is supported by the Strong Motion Instrumentation Program, California Division of Mines and Geology. The authors are grateful for this support. The authors are also grateful to Bob Darragh, Moh-Jiann Huang, Praveen Malhotra, and Anthony Shakal for providing structural plans and earthquake records and Pat Hipley for assisting with implementation of the CALTRANS procedure for computing abutment stiffness. Any opinion, discussion, and conclusions are those of the authors and do not necessarily reflect the views of the sponsor.

REFERENCES

AASHTO-83. (1988). *Guide Specifications for Seismic Design of Highway Bridges,* American Association of State Highway and Transportation Officials, Washington, D.C.

ATC-6. (1981). *Seismic Design Guidelines for Highway Bridges*, Applied Technology Council, Berkeley, CA, October.

CALTRANS. (1990). *Bridge Design Specifications,* California Department of Transportation, Sacramento, CA, June.

CALTRANS. (1989). *Bridge Design Aids 14-1*, California Department of Transportation, Sacramento, CA, October.

CALTRANS. (1988). *Memo to Designers 5-1,* California Department of Transportation, Division of Structures, Sacramento, CA, September.

Gates, J. H. and Smith, M. J. (1982). *Verification of Dynamic Modeling Method by Prototype Excitation,* FHWA/CA/SD-82/07, California Department of Transportation, Office of Structures Design, Sacramento, California, November.

Goel, R. K. and Chopra, A. K. (1990). *Inelastic Seismic Response of One-Story, Asymmetric-Plan Systems,* Report No. UCB/EERC-90/14, Earthquake Engineering Research Center, University of California, Berkeley, California, October.

Jennings, P. C. and Wood, J. H. (1971). "Earthquake Damage to Freeway Structures," *Engineering Features of the San Fernando Earthquake*, Report No. EERL 71-02, Earthquake Engineering Research Laboratory, California Institute of Technology, Pasadena, CA.

Romstad, K. and Maroney, B. (1990). *Interpretation of Painter Street Overcrossing Records to Define Input Motions to the Bridge Superstructure*, Final Report to Department of Conservation, Division of Mines and Geology, Office of Strong Motion Studies, October.

Shakal, A. F., et al. (1992). *CSMIP Strong-Motion Records from the Petrolia, California Earthquakes of April 25-26, 1992*, Report No. OSMS 92-05, California Department of Conservation, Division of Mines and Geology, Office of Strong Motion Studies, May 20.

Sweet, J. and Morrill, K. B. (1993). "Nonlinear Soil-Structure Interaction Simulation of the Painter Street Overcrossing," *Proceedings of the Second Annual Caltrans Seismic research Workshop*, Sacramento, CA, March 16-18.

Tsai, N. C. et al. (1993). *Application of CALTRANS' Current Seismic Evaluation Procedures to Selected Short Bridge Overcrossing Structures,* Technical Report, Dames and Moore, Oakland, CA, June.